Journal of Inflammation Research

Dovepress
Taylor & Francis Group

Open Access Full Text Article

ORIGINAL RESEARCH

Cordyceps Sinensis Reduces Inflammation and Protects BEAS-2B Cells From LPS-Induced THP-1 Cell Injury

Xiaqing Wu[1,2,*], Xin Li[2,*], Ying Chai[1,2], Yushan Tian[1,2], Hongjuan Wang[1,2], Xiao Li[1,2], Jingzheng Zhang[2], Chunmei Guang[2], Enliang Hong[2], Haoping Cheng[2], Qingyuan Hu[1,2], Huan Chen[1,2], Hongwei Hou[1,2]

[1]Key Laboratory of Tobacco Biological Effects, China National Tobacco Quality Supervision & Test Center, Zhengzhou, Henan, People's Republic of China; [2]Beijing Life Science Academy, Beijing, People's Republic of China

*These authors contributed equally to this work

Correspondence: Huan Chen; Hongwei Hou, Key Laboratory of Tobacco Biological Effects, China National Tobacco Quality Supervision & Test Center, New & High-tech Industry Development Zone, No.6 Cuizhu Street, Zhengzhou, Henan, 450001, People's Republic of China, Email hunny_ch@163.com; qsfctc@163.com

Introduction: Cordyceps sinensis, an entomogenous fungus with unique biological properties, has demonstrated significant anti-inflammatory potential. However, its effects on inflammation regulation need to be further investigated in detail.

Methods: In this study, we aimed to analyze the Cordyceps sinensis extract (CSE) obtained via ethanol extraction and to assess its effects on inflammation regulation. The secretion of pro-inflammatory cytokines (IL-6, TNF-α, IL-8, and IL-1β) and the level of MMP9, Nrf2/HO-1 and ROS were evaluated. A transwell system with THP-1 and BEAS-2B cells was used to explore the inflammatory damage. Gene ontology (GO) and Kyoto encyclopedia of genes and genomes (KEGG) enrichment analyses were conducted on the differentially expressed genes.

Results: CSE exhibited no cytotoxicity to THP-1 cells at concentrations ≤ 1.6 mg/mL. Treatment of LPS-induced THP-1 cells with CSE significantly inhibited the secretion of pro-inflammatory cytokines. CSE reduced inflammation-related protein MMP9, while upregulating the anti-inflammatory Nrf2/HO-1 signaling pathway. Fluorescence assays using DCF and JC-1 further confirmed that CSE help mitigate oxidative stress-induced inflammation. CSE treatment protected BEAS-2B cells from inflammatory damage. Moreover, the immune system process was a shared GO term between LPS-only treatment and combined LPS and CSE treatment. KEGG enrichment analysis showed that CSE is capable of regulating genes associated with inflammatory and anti-inflammatory responses.

Conclusion: These findings highlight the potential of CSE as an immune-regulating agent in functional foods and health products.

Keywords: Cordyceps sinensis, anti-inflammatory, macrophage, transcriptomic analyses

Introduction

Natural products are rich sources of bioactive compounds known for their therapeutic efficacy and safety profile.[1] Traditional Chinese medicines play significant roles in alleviating various complex diseases and promoting physical health due to their unique pharmacological effects.[2–4] Among these, Cordyceps sinensis (C. sinensis)—a member of the Cordycipitaceae family—is an entomogenous fungus that grows on insect larvae and has long been used as a tonic in traditional Chinese medicine.[5–9] Ancient texts document its effectiveness in relieving cough, alleviating asthma, clearing the lungs, and resolving phlegm.[4,9,10] Recent research has demonstrated that extracts of C. sinensis possess antioxidant, anti-inflammatory, and antibacterial activities, suggesting their potential for biomedical applications.[11] Its bioactive components, including nucleosides, polysaccharides, sterols, proteins, and peptides, contribute to its therapeutic effects. For example, nucleosides serve as quality control markers and exhibit anti-inflammatory, anti-cancer, anti-fibrotic, and

Received: 26 November 2024
Accepted: 2 March 2025
Published: 19 March 2025

cardioprotective effects, while polysaccharides and peptides can modulate immune cell activities and protect against oxidative injury.[4,12–18] Modern pharmacological studies have demonstrated that Cordyceps sinensis and its constituents possess antioxidative, immune-regulating, and metabolic-regulating properties.[4,19–22]

Air pollution, dust, soot, trauma, and infection are important causes of lung diseases.[23–26] Inflammation, a hallmark of lung diseases, orchestrates disease progression and therapeutic outcomes by driving immune dysregulation.[27] Early immune surveillance involves rapid recruitment of macrophages and neutrophils to combat infections.[28] However, persistent activation of these cells exacerbates tissue damage through excessive cytokine release (eg, IL-1β, TNF-α) and oxidative stress.[29,30] Notably, macrophage polarization dynamically shifts during infection—from pro-inflammatory M1 phenotypes in acute phases to reparative M2 phenotypes promoting resolution.[31] The Nrf2/HO-1 pathway further modulates oxidative injury by neutralizing reactive oxygen species (ROS) triggered by environmental toxins or microbial components like LPS.[32] While Cordyceps sinensis has shown promise in ameliorating renal ischemia-reperfusion-induced lung injury via AMPK/mTOR-mediated autophagy,[33] its precise mechanisms in inflammatory lung disorders remain elusive.

Here, we prepared Cordyceps sinensis ethanol extract (CSE), characterized its composition via LC-MS, and evaluated its anti-inflammatory and antioxidant efficacy in THP-1 macrophages. CSE pretreatment significantly attenuated LPS-induced oxidative stress, as evidenced by reduced DCF fluorescence (ROS levels decreased by 40%) and restored mitochondrial membrane potential (JC-1 red/green ratio increased 1.8-fold). RT-qPCR revealed dose-dependent down-regulation of pro-inflammatory genes (IL-1β, TNF-α; $p<0.01$) and upregulation of Nrf2 (>2-fold). In a transwell co-culture model, CSE-treated THP-1 cells mitigated LPS-driven inflammatory damage to BEAS-2B bronchial epithelia, reducing IL-8 secretion by 55%. Transcriptomic profiling identified 342 differentially expressed genes in CSE-exposed cells, with KEGG enrichment highlighting Toll-like receptor and NF-κB pathways. Functional validation confirmed CSE's suppression of NF-κB nuclear translocation via AMPK activation. These findings position CSE as a multifaceted modulator of inflammation and oxidative stress, supporting its potential as a functional food ingredient for respiratory health.

Materials and Methods

Reagent and Antibodies

Cordyceps sinensis was purchased from Beijing Tongrentang Co., Ltd., (Beijing, China). We obtained Roswell Park Memorial Institute 1640 medium (RPMI-1640) from Gibco Invitrogen (California, USA). The Cell Counting Kit-8 (CCK-8) for detecting cytotoxicity was sourced from Tongren Chemistry (Japan). We procured the Annexin V-FITC apoptosis detection kit and the fluorescence probe DCFH-DA from Beyotime (Shanghai, China). ELISA kits were purchased from Elabscience (Wuhan, China). We obtained lipopolysaccharides (LPS) from GLPBIO (US) and BEGM medium from Lonza (Basel, Switzerland). The THP-1 special medium came from Pricella (Wuhan, China).

Cell Lines and Culture

THP-1 macrophages: Cells (Pricella, China, Cat. No. CL-0233) were maintained in RPMI-1640 medium supplemented with 10% fetal bovine serum (FBS; Gibco, Cat. No. 10099141C), 100 U/mL penicillin, and 100 μg/mL streptomycin (Gibco, Cat. No. 15140122) at 37°C under 5% CO_2. For differentiation, THP-1 monocytes (1×10^5 cells/mL) were treated with 100 ng/mL phorbol 12-myristate 13-acetate (PMA; MedChemExpress, Cat. No. HY-18739) for 48 h.

BEAS-2B bronchial epithelial cells: Cells (Pricella, Cat. No. CL-0496) were cultured in BEGM medium (Lonza, Cat. No. CC-3170) under identical conditions.

Cell Viability

CCK-8 assay: Differentiated THP-1 macrophages were seeded in 96-well plates (1×10^5 cells/well) and treated with Cordyceps sinensis extract (CSE; 0.1–100 μg/mL) or vehicle (0.1% DMSO) for 24 h. CCK-8 reagent (10% v/v) was added to each well, followed by incubation at 37°C for 2 h. Absorbance at 450 nm was measured using a FlexStation 3 microplate reader (Molecular Devices, USA). Cell viability (%) was normalized to untreated controls.

Quantification by ELISA

Cytokine quantification: Cell culture supernatants were centrifuged (300 ×g, 10 min) to remove debris. Levels of TNF-α, IL-1β, IL-6, IL-8 were quantified using commercial ELISA kits according to manufacturers' protocols. Standard curves were generated using serial dilutions of recombinant proteins, and cytokine concentrations (pg/mL) were interpolated from absorbance values (450 nm).

RNA Extraction and Real-Time PCR

Gene expression analysis: Total RNA was isolated using the SteadyPure Universal RNA Extraction Kit (AG, China, Cat. No. AG21023). cDNA synthesis was performed with 500 ng RNA using HiScript III Reverse Transcriptase (Vazyme, China, Cat. No. R323-01). Quantitative PCR was conducted using ChamQ SYBR qPCR Master Mix (Vazyme, Cat. No. Q311-02) on a QuantStudio 5 system (Thermo Fisher, USA). Relative mRNA levels were calculated via the 2-ΔΔCT method.

ROS Production and Mitochondrial Membrane Potential

ROS detection: Differentiated THP-1 cells were loaded with 10 μM DCFH-DA in serum-free medium for 30 min. Fluorescence (Ex/Em: 488/525 nm) was quantified using a Cytation 5 plate reader (BioTek, USA).

Mitochondrial membrane potential: Cells were stained with 5 μg/mL JC-1 (Invitrogen, Cat. No. M34152) for 20 min. The red/green fluorescence ratio (Ex/Em: 488/590 nm vs 488/530 nm) was analyzed to assess mitochondrial health.

MMP9 Expression by Western Blot

Western blotting: Total proteins were extracted using RIPA buffer (Beyotime, Cat. No. P0013B) containing protease inhibitors. Protein concentrations were determined via BCA assay (Thermo Fisher, Cat. No. 23225). Samples (20 μg/lane) were resolved on 10% SDS-PAGE gels and transferred to PVDF membranes (Millipore, USA). After blocking with 5% non-fat milk, membranes were incubated overnight with primary antibodies at 4°C, followed by HRP-conjugated secondary antibodies (1:5000; Proteintech, Cat. No. SA00001-2) for 1 h at RT. Bands were visualized using ECL reagent (Beyotime, Cat. No. P0018FS) and quantified via ImageJ (NIH).

Transcriptome Analysis Sample Preparation and Differential Analysis

RNA sequencing and bioinformatics: Total RNA from THP-1 cells (n=3 per group: Control, LPS, LPS+CSE) was extracted, and libraries were prepared using the NEBNext Ultra II RNA Kit (NEB, USA). Sequencing was performed on an Illumina NovaSeq 6000 platform (150 bp paired-end). Raw reads were filtered using SOAPnuke (v2.1.0) to remove adapters, low-quality reads (Q20 < 95%), and reads with >5% N bases. Differentially expressed genes (DEGs) were identified using DESeq2 (v1.4.5;). GO and KEGG enrichment analyses were performed with clusterProfiler (v4.0).

GO Enrichment and KEGG Pathways Enrichment Analysis

GO enrichment is a globally recognized method for categorizing gene functions, serving as a standardized system for gene functional classification. Typically, the Gene Ontology (GO) framework encompasses three distinct aspects: cellular component, molecular function, and biological process. In the study, genes affected by LPS and LPS+CSE in THP-1 cells were aligned with their corresponding terms in the GO database. The frequency of genes associated with each term was then determined. Subsequently, the GO terms were organized and ranked based on the gene count, culminating in the identification of the top 30 GO terms. KEGG, is an additional genomic information database designed for systematic analysis of gene functions. It facilitates the comprehensive investigation of gene expressions within the context of entire networks. Parallel to the GO enrichment analysis, the top 20 KEGG pathways were identified, screened, and ordered according to the number of differentially expressed genes.

Statistical Analysis

Statistical analysis: Data are presented as mean ± SEM from ≥3 independent experiments. One-way ANOVA with Tukey's post-hoc test was used for multi-group comparisons. A p-value <0.05 was considered statistically significant.

Results

Identification of CSE

CSE was prepared through ethanol extraction, followed by concentration, centrifugation, and lyophilization. LC-MS analysis of multiple batches revealed consistent chemical profiles (Figure 1), with nucleosides identified as the primary components. The absence of batch-to-batch variability confirmed the stability of CSE for experimental use.

Cell Viability of CSE on THP-1 Cells

THP-1 cells were selected to evaluate the anti-inflammatory effects of CSE. CCK-8 assays demonstrated no cytotoxicity at concentrations up to 1600 μg/mL (Figure 2), confirming its safety for subsequent experiments.

Inflammatory Inhibition in LPS-Induced THP-1 Cells by CSE

To evaluate the anti-inflammatory effects of CSE, we measured the levels of proinflammatory cytokines in LPS-induced THP-1 cells using enzyme-linked immunosorbent assay (ELISA). Considering the in vivo research in future and the dose conversion formula, the study selected a CSE concentration range of 12.5–50 μg/mL. As shown in Figure 3A and B, D, CSE significantly reduced the concentrations of IL-6 and TNF-α in the supernatant of LPS-induced THP-1 cells. Rutin is a natural anti-inflammatory compound and dexamethasone (Dex) is a commercially available anti-inflammatory drug, which

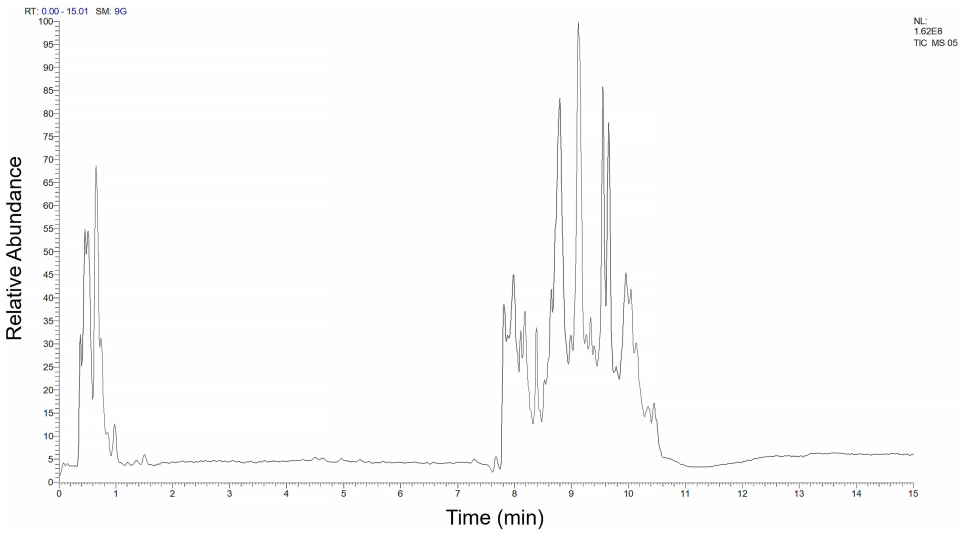

Figure 1 Total ion chromatography of CSE.

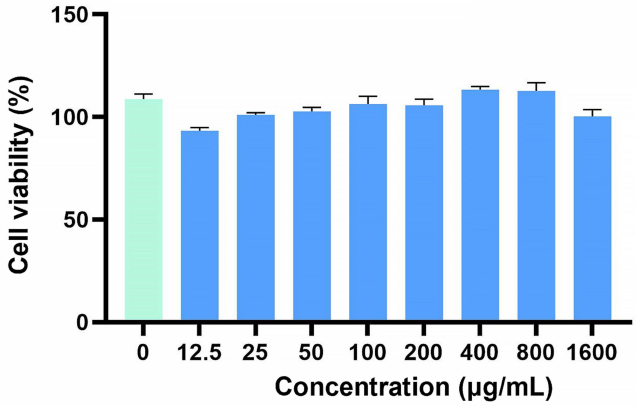

Figure 2 THP-1 cell viability when treated with different concentrations of CSE for 24h.

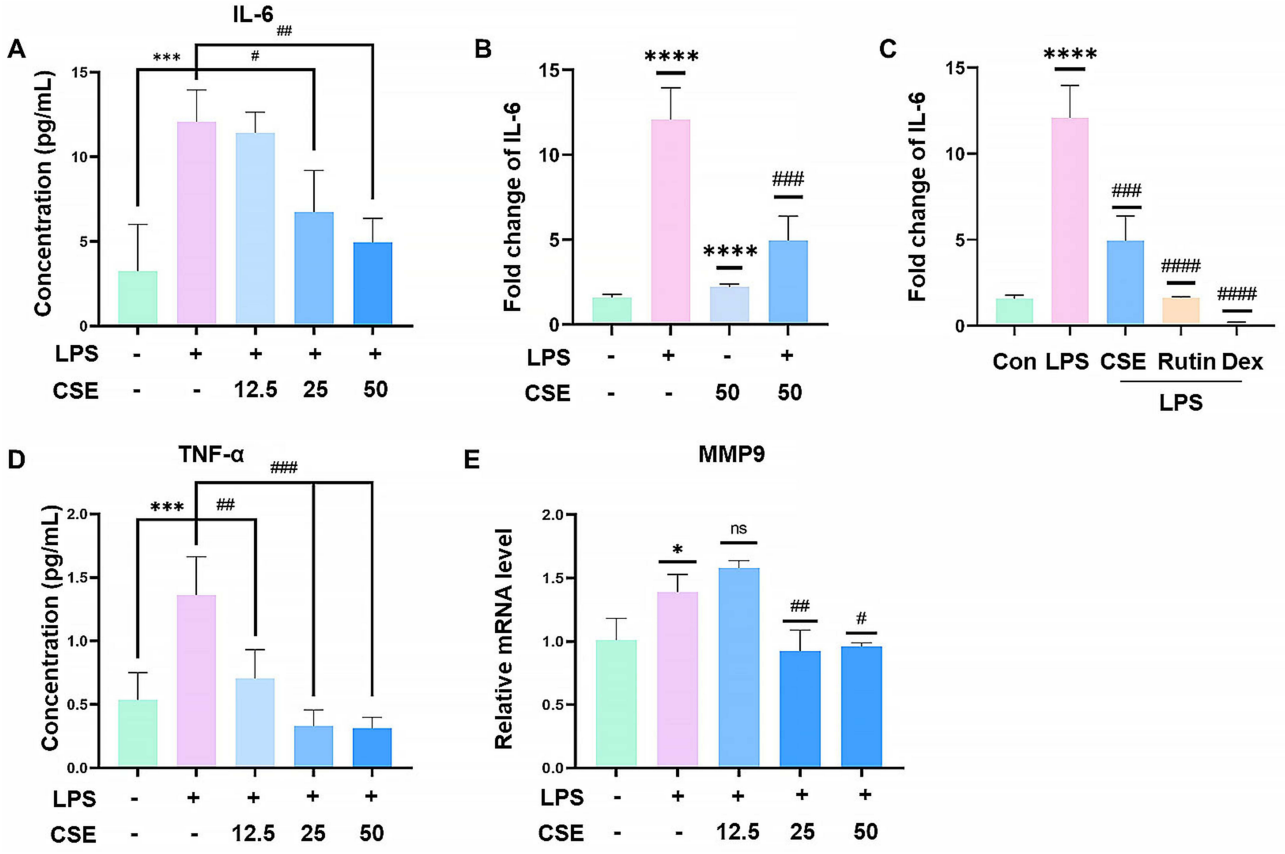

Figure 3 Regulation of CSE on inflammatory cytokines. Secretion levels of IL-6 (**A**) and TNF-α (**D**) in THP-1 cells after treatment with different concentrations of CSE in the presence of LPS. (**B**) Fold change of IL-6 in THP-1 cells under different conditions. (**C**) Fold change of IL-6 in LPS induced THP-1 cells with pretreatment of CSE (50 μg/mL), Rutin (50 μM), Dex (10 μM). (**E**) mRNA level of MMP9 in THP-1 cells after treatment with different concentrations of CSE in the presence of LPS. THP-1 cells were pre-treated with CSE (12.5μg/mL, 25μg/mL and 50μg/mL) for 24 h. After pre-treatment, LPS (10 μg/mL) was treated for another 2 h. Statistical analyses comparing with the control group are denoted as follows: *$p < 0.05$, ***$p < 0.001$, ****$p < 0.0001$. Statistical analyses comparing with the LPS-treated group are denoted as follows: $^{\#}p < 0.05$, $^{\#\#}p < 0.01$, $^{\#\#\#}p < 0.001$, $^{\#\#\#\#}p < 0.0001$. "ns" presents no significant difference.

have been widely used in clinical application and basic research. Figure 3C shows that CSE exhibits similar effects to rutin and Dex in inhibiting IL-6, indicating CSE's effectiveness in anti-inflammatory activity. The anti-inflammatory effect was dose-dependent, with greater inhibition observed at higher concentrations of CSE. For IL-6, The difference in IL-6 between the 25μg/mL, 50μg/mL group and the LPS groups was significant ($p < 0.05$, $p < 0.01$), while the difference between the 12.5μg/mL group and the LPS groups was non-significant ($p > 0.05$). The difference in TNF-α between the 12.5 μg/mL group and the LPS group was significant ($p < 0.01$), while the differences in the 25 μg/mL and 50 μg/mL groups compared to the LPS group were even more significant ($p < 0.001$). MMP9, a protein expressed in inflammatory cells that regulates inflammation in tissues and diseases, was also examined. As depicted in Figure 3E, LPS stimulation increased MMP9 expression in THP-1 cells; however, after 24 hours of CSE treatment, the mRNA levels of MMP9 were significantly decreased ($p < 0.01$ for the 25μg/mL group, $p < 0.05$ for the 50μg/mL group), indicating transcriptional downregulation and supporting the anti-inflammatory properties of CSE.

Inhibition of LPS-Induced ROS Production in THP-1 Cells by CSE

We next assessed the effect of CSE on oxidative stress in THP-1 cells using the H_2DCF fluorescent probe. As shown in Figures 4A and C, LPS stimulation significantly increased reactive oxygen species (ROS) production, which was evident from the enhanced green fluorescence intensity compared to the control group. After 24 hours of CSE treatment at concentrations of 12.5, 25, and 50 μg/mL ($p < 0.001$), ROS production was notably suppressed. Furthermore, changes in mitochondrial membrane potential were evaluated using the JC-1 fluorescent probe. Figures 4B and D demonstrate that LPS stimulation led to a decrease ($p < 0.01$) in mitochondrial membrane potential, with JC-1 predominantly existing as

https://doi.org/10.2147/JIR.S508098

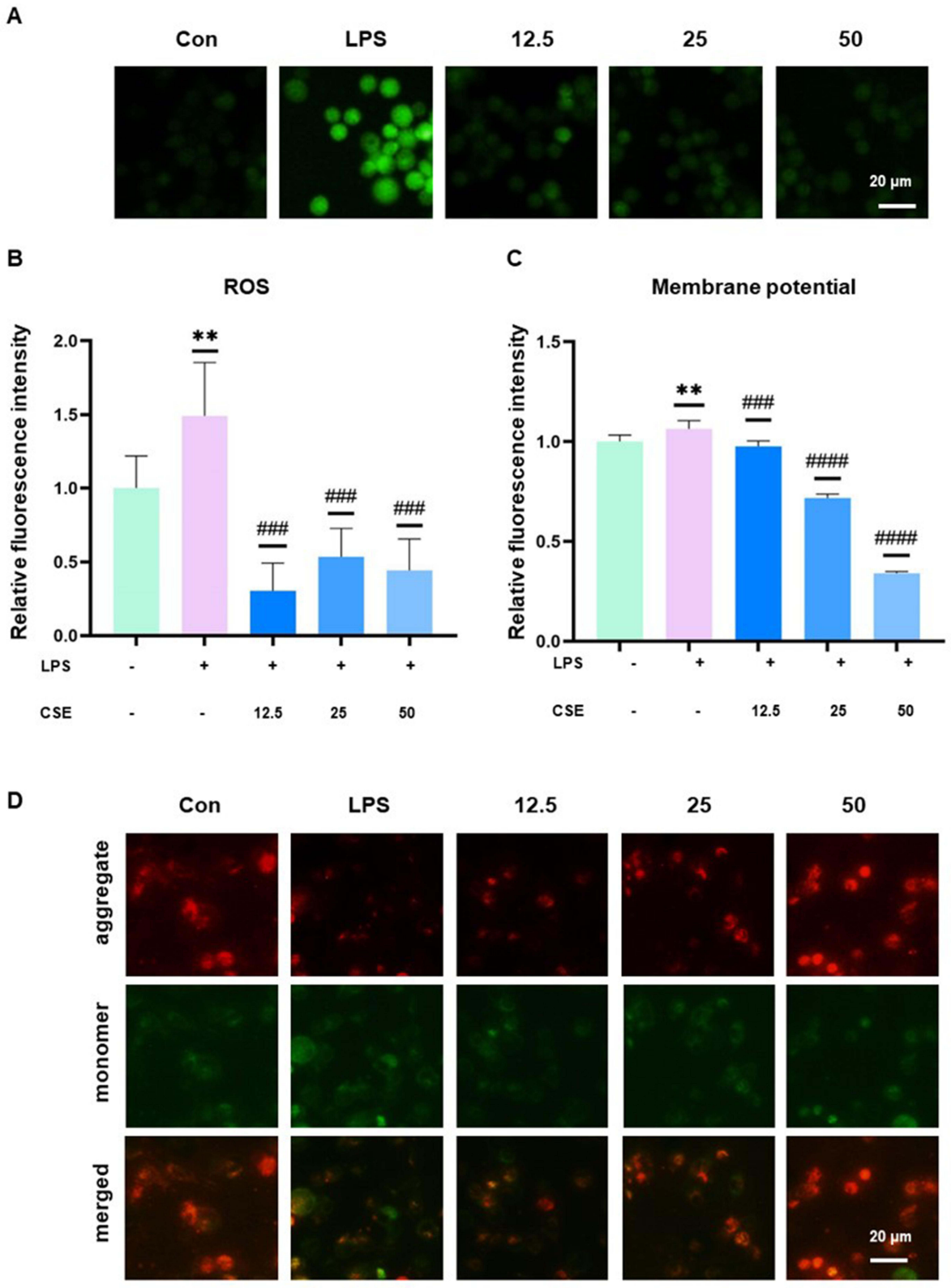

Figure 4 Regulation of CSE on LPS-induced oxidative stress in THP-1 cells. Fluorescence images (**A**) and quantification (**B**) of DCF in LPS-induced THP-1 cells after CSE treatment. Fluorescence quantification (**C**) and images (**D**) of JC-1 in LPS-induced THP-1 cells after CSE treatment. The concentration of CSE used was 12.5 μg/mL, 25 μg/mL, and 50 μg/mL. After 24 h of CSE pre-treatment, LPS (10 μg/mL) was treated for another 2 h. Statistical analyses comparing with the control group are denoted as follows: $^{**}p < 0.01$. Statistical analyses comparing with the LPS-treated group are denoted as follows: $^{\#\#\#}p < 0.001$, $^{\#\#\#\#}p < 0.0001$.

a monomer—resulting in increased green fluorescence and decreased red fluorescence. However, CSE treatment restored red fluorescence in LPS-induced THP-1 cells ($p < 0.001$ for the 12.5μg/mL group, $p < 0.0001$ for the 25μg/mL group, $p < 0.0001$ for the 50μg/mL group), indicating an improvement in mitochondrial function.

Modulation of Inflammatory Cytokines and Activation of the Nrf2/HO-1 Pathway by CSE

We assessed the mRNA expression levels of the proinflammatory cytokines IL-6, TNF-α, IL-8, and IL-1β in LPS-induced THP-1 cells following CSE treatment. The results (Figures 5A–D) confirmed that CSE downregulated the expression of these cytokines at the transcriptional level, which supports its anti-inflammatory effects. Additionally, because the Nrf2/HO-1 pathway plays a critical role in mediating anti-inflammatory responses, we measured the mRNA

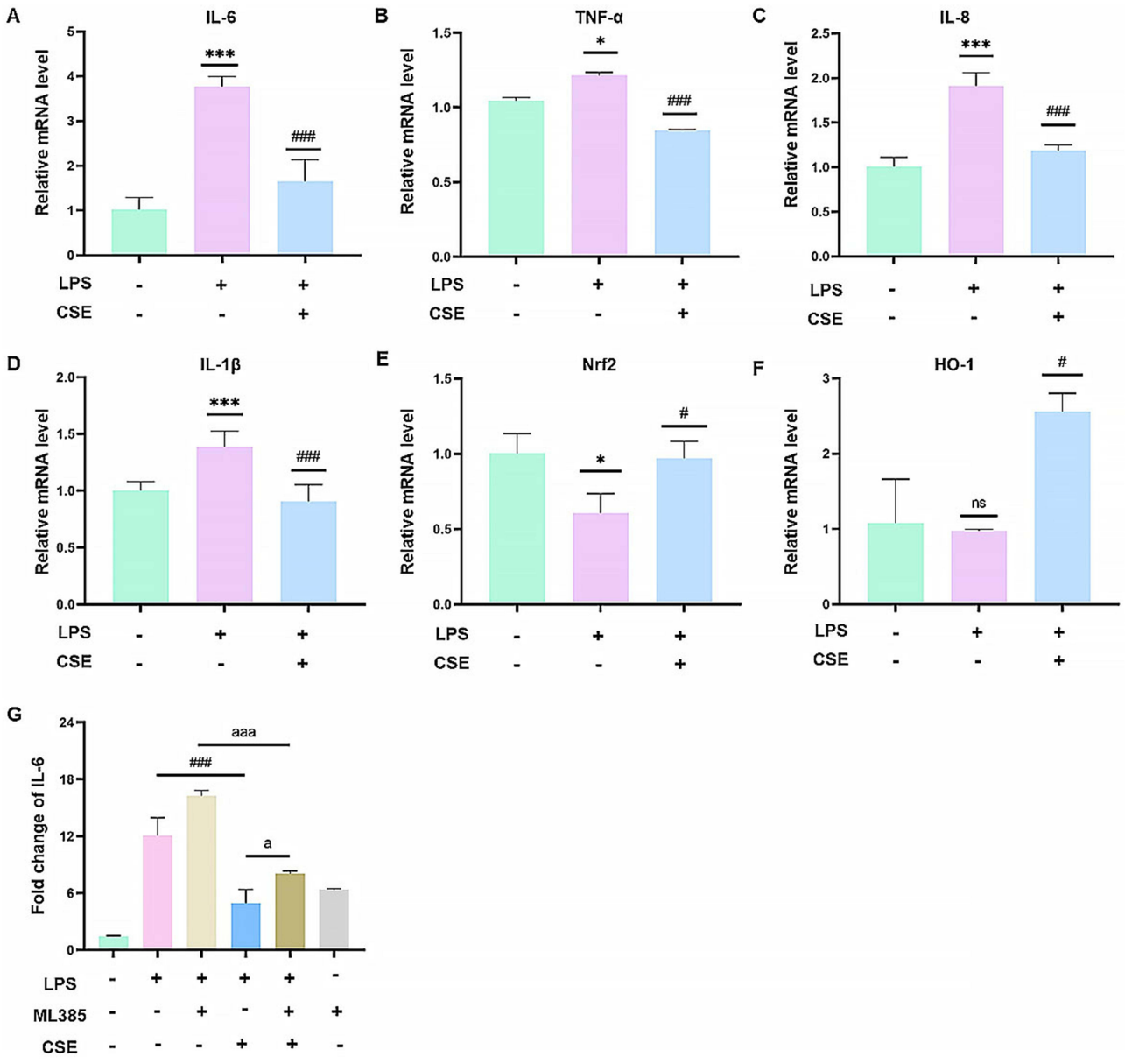

Figure 5 Regulation of CSE on expression of inflammation-related proteins. mRNA level of IL-6 (**A**), TNF-α (**B**), IL-8 (**C**), and IL-1β (**D**) in THP-1 cells after LPS treatment in the presence or absence of CSE. mRNA level of Nrf2 (**E**) and HO-1 (**F**) in THP-1 cells after LPS treatment in the presence or absence of CSE. (**G**) Fold change of IL-6 in THP-1 cells under different conditions. The concentration of ML385 was 5 μM. The concentration of CSE was 50 μg/mL. THP-1 cells were pre-treated with CSE for 24 h. After pre-treatment, LPS (10 μg/mL) was treated for another 2 h. Statistical analyses comparing with the control group are denoted as follows: *$p < 0.05$, ***$p < 0.001$. Statistical analyses comparing with the LPS-treated group are denoted as follows: #$p < 0.05$, ###$p < 0.001$. Statistical analyses comparing with the CSE+ML385+LPS-treated group are denoted as follows: $^{a}p < 0.05$, $^{aaa}p < 0.001$. "ns" presents no significant difference.

https://doi.org/10.2147/JIR.S508098

levels of Nrf2 ($p < 0.05$) and HO-1 ($p < 0.05$). As shown in Figures 5E and F, CSE exposure resulted in a statistically significant increase in the expression of these genes compared to the LPS group. In Figures 5G, ML385, the inhibitor of Nrf2, significantly diminished the decrease of IL-6 levels induced by CSE in LPS induced THP-1 cells ($p < 0.05$). These findings suggest that CSE treatment performs the anti-inflammatory capacity of THP-1 cells.

CSE Treatment Inhibited Inflammatory Injury in BEAS-2B Cells

A transwell system was employed to further investigate the inhibitory effect of CSE on inflammatory injury in BEAS-2B cells. Prior to the experiment, we confirmed that CSE was non-cytotoxic to BEAS-2B cells. THP-1 cells were seeded in the upper compartment of the transwell, while BEAS-2B cells were cultured in the lower compartment (Figure 6A). CSE was added to the medium in the upper compartment. After incubation, we assessed both apoptosis and inflammatory status in the BEAS-2B cells. As shown in Figure 6B, cell viability was restored, as indicated by a reduction ($p < 0.0001$) in Annexin V fluorescence intensity. Additionally, IL-6 levels in the lower compartment were significantly reduced in the CSE-treated group compared to the LPS-treated group ($p < 0.001$) (Figure 6C).

Widespread GO and KEGG Pathway Enrichment Analysis of Transcriptome Changes Induced by CSE Administration on LPS Treated THP-1 Cells

RNA-Seq combined with bioinformatics analysis was used to characterize alterations in gene expression triggered by LPS-induced inflammation and CSE pretreatment. Differentially expressed genes (DEGs) were identified using DESeq2 with a threshold of q value < 0.05 and $\log_2FC \geq 1$. Analysis revealed significant alterations in the expression of 1359 genes between the PBS control and LPS-treated groups. As depicted in Figure 7A, the volcano plot shows that 863 genes were upregulated and 496 were downregulated by LPS compared to PBS samples. Comparison between the LPS-treated group and the LPS+CSE-treated group identified a total of 670 DEGs (382 upregulated and 288 downregulated; Figure 7B). A Venn diagram (Figure 7C) illustrates that 292 genes were commonly regulated by both LPS and LPS +CSE treatments.

To understand the biological significance of these DEGs, GO enrichment analysis was performed (Figures 7D and E). For the LPS treatment, the top 10 GO terms in the categories of cellular component (CC), molecular function (MF), and biological process (BP) included cytosol, extracellular exosome, protein binding, identical protein binding, inflammatory response, and cellular response to lipopolysaccharide. In the LPS+CSE treatment, the top 30 GO terms included cytosolic ribosome, ribosome, structural constituent of ribosome, RNA binding, cytoplasmic translation, and SRP-dependent cotranslational protein targeting to membrane. Comparing the top 30 GO terms between PBS vs LPS and LPS+CSE vs LPS, 10 terms were found to be identical (3 in CC, 3 in MF, and 4 in BP), with "immune system process" being a common term related to biological processes.

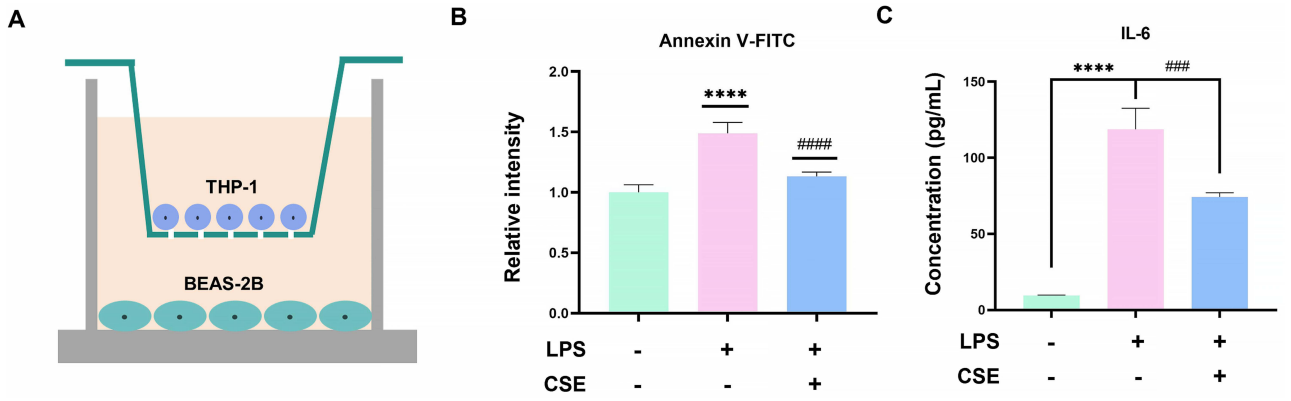

Figure 6 Inhibition of CSE on inflammatory injuries in BEAS-2B cells. (**A**) Transwell system. (**B**) Relative fluorescence quantification of Annexin V-FITC in BEAS-2B cells under different conditions. (**C**) Concentration of IL-6 in the bottom layer of BEAS-2B cells under different conditions. After 24 h of CSE (50 μg/mL) pre-treatment, LPS (10 μg/mL) was added in the culture medium of the upper layer for another 2 h. Statistical analyses comparing with the control group are denoted as follows: ****$p < 0.0001$. Statistical analyses comparing with the LPS-treated group are denoted as follows: ###$p < 0.001$, ####$p < 0.0001$.

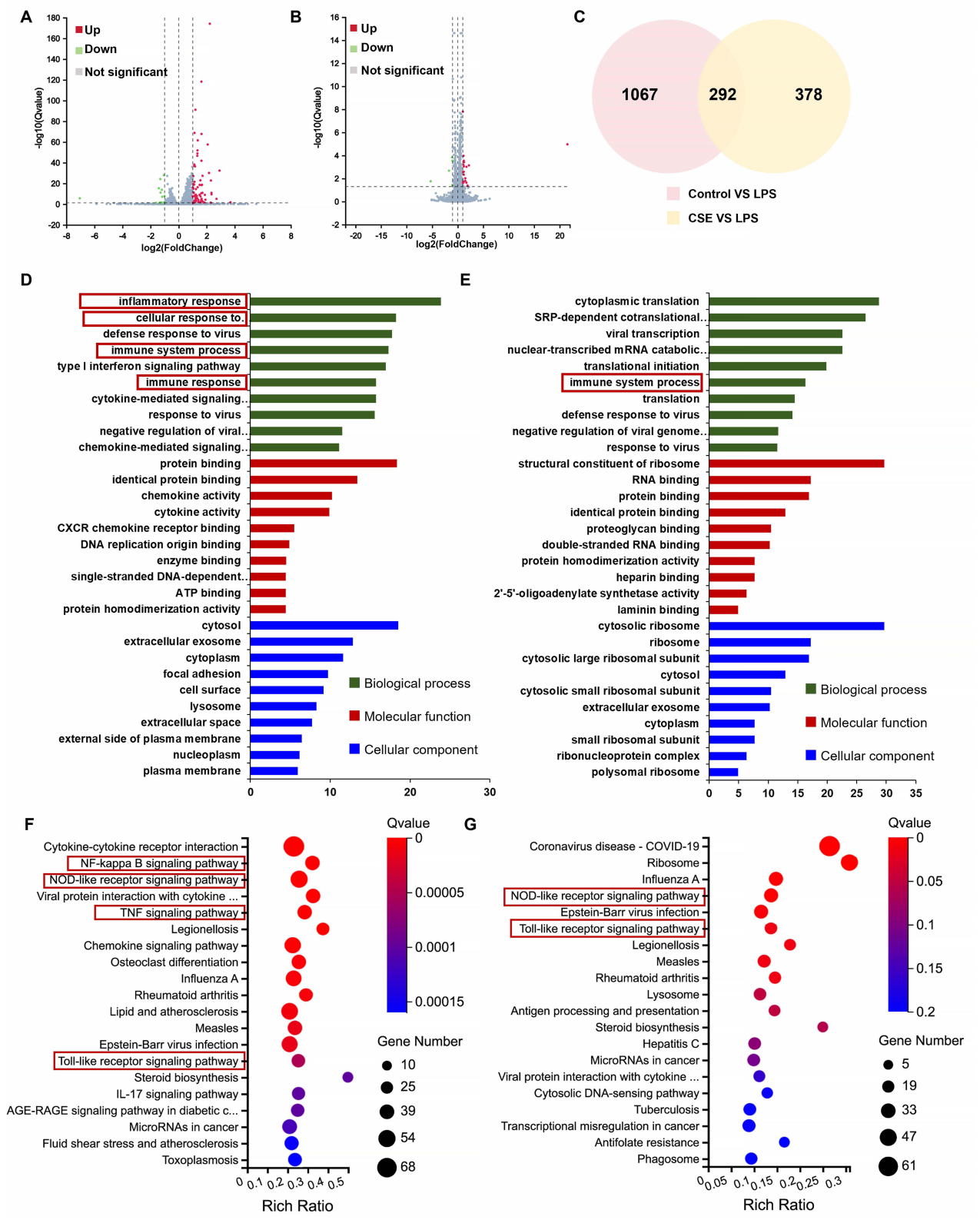

Figure 7 Differential gene analysis about change and enrichment. (**A** and **B**) Volcano plots were depicted with –log10 (Qvalue) against log2 (FoldChange) of PBS vs LPS's and CSE vs LPS's comparation. (**C**) The number of differential expressed genes related to PBS vs LPS's and CSE vs LPS's comparation. GO enrichment classification histogram in THP-1 cells under the influence of LPS (**D**) and LPS +CSE (**E**). KEGG enrichment bubble chart in THP-1 cells under the influence of LPS (**F**) and LPS +CSE (**G**).

https://doi.org/10.2147/JIR.S508098

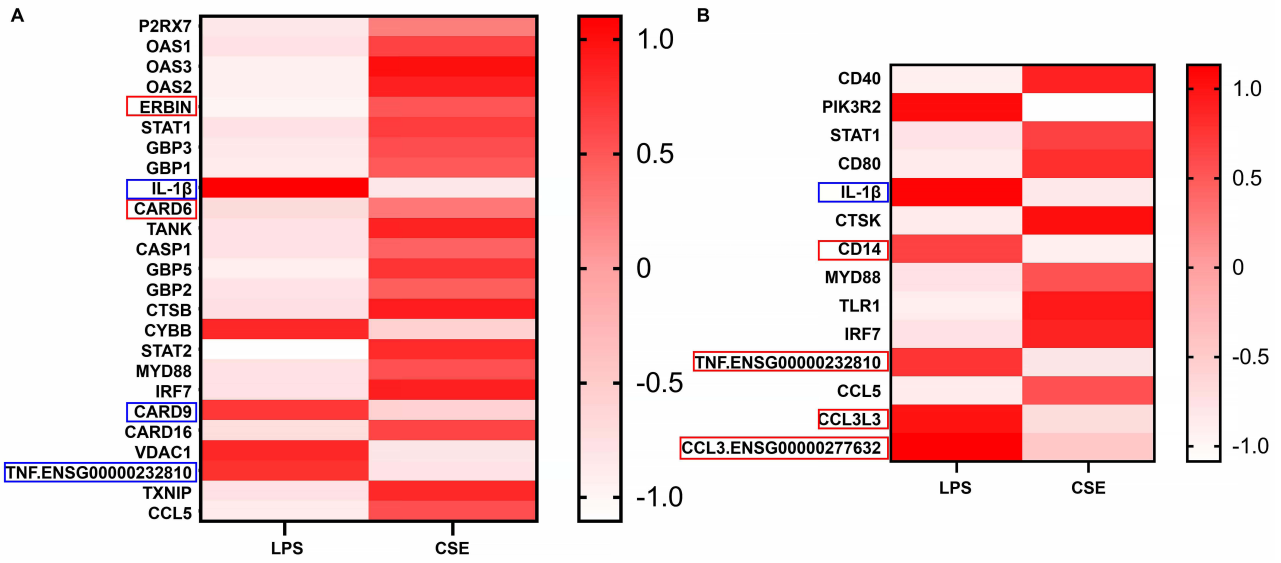

Figure 8 Differential expressed genes' numbers in the NOD-like receptor signaling pathway and Toll-like receptor signaling pathway. The log of induction folds of identical genes changed by CSE treatment in NOD-like receptor signaling pathway (**A**) and Toll-like receptor signaling pathway (**B**). CCL3.ENSG000002 is the Ensembl gene ID for the CCL3 gene. TNF.ENSG00000232810 is the Ensembl gene ID for the TNF-α gene.

A total of 1359 and 670 DEGs were mapped to the KEGG database with a significance level of $p \leq 0.05$ for the PBS vs LPS and LPS+CSE vs LPS comparisons, respectively (Figures 7F and G). Pathway analysis revealed that, in comparison to PBS, the LPS-treated group showed significant enrichment in the NF-κB signaling pathway, NOD-like receptor signaling pathway, and TNF signaling pathway. In contrast, the comparison of the CSE-treated group with the LPS group showed significant enrichment of the NOD-like receptor and Toll-like receptor signaling pathways, both of which are associated with inflammation.

Differential Gene Analysis Related to NOD-Like Receptor Signaling Pathway and Toll-Like Receptor Signaling Pathway

In THP-1 cells, the number of DEGs related to the NOD-like receptor signaling pathway was 47 in the PBS vs LPS comparison and 25 in the LPS+CSE vs LPS comparison. As shown in Figure 8A, key cytokine genes (IL-1β and TNF-α) were significantly downregulated following CSE treatment, consistent with our experimental results. In addition, genes associated with anti-inflammatory responses (eg, CARD6, ERBIN) were significantly upregulated when comparing the CSE group with the LPS group. Similarly, for the Toll-like receptor signaling pathway, 26 and 14 DEGs were identified in the PBS vs LPS and LPS+CSE vs LPS comparisons, respectively. As depicted in Figure 8B, several pivotal genes associated with inflammatory responses (eg, CCL3L3, CCL3.ENSG00000232810, CD14) were significantly down-regulated in the CSE-treated group compared to the LPS group.

Discussion

Our study demonstrates that Cordyceps sinensis extract (CSE) attenuates LPS-induced inflammation in THP-1 macrophages through multifaceted mechanisms, including suppression of pro-inflammatory cytokines, mitigation of oxidative stress, and activation of the Nrf2/HO-1 antioxidant pathway. These findings align with the traditional use of Cordyceps sinensis in managing inflammatory conditions and provide mechanistic insights into its potential as a functional food ingredient.[4,34,35]

The robust reduction in IL-6, TNF-α, IL-1β, and IL-8 levels—both at the protein and transcriptional levels—highlights CSE's capacity to disrupt key inflammatory cascades.[36] TNF-α and IL-1β are central drivers of neutrophilic inflammation and tissue remodeling in chronic lung diseases, while IL-8 promotes neutrophil recruitment and protease-mediated tissue damage. By suppressing these cytokines, CSE may interrupt the self-perpetuating cycle of inflammation and oxidative stress observed in pathologies like COPD (Chronic Obstructive Pulmonary Disease) and ARDS (Acute Respiratory Distress Syndrome).[37–40] The

downregulation of MMP9, a protease critical to extracellular matrix degradation, further underscores CSE's role in preserving tissue integrity during inflammation.[41–45]

CSE's antioxidant effects were evident in its ability to reduce ROS accumulation and restore mitochondrial membrane potential. Excessive ROS not only amplifies inflammatory signaling but also exacerbates mitochondrial dysfunction, a hallmark of chronic inflammatory diseases.[46–48] The activation of the Nrf2/HO-1 pathway by CSE likely contributes to this protective effect, as Nrf2 is a master regulator of cellular antioxidant responses.[49,50] This aligns with studies showing that natural compounds, such as cordycepin and plant polysaccharides, mitigate oxidative damage via Nrf2 activation.[51,52]

Transcriptomic analysis further elucidated CSE's immunomodulatory mechanisms. The enrichment of Toll-like and NOD-like receptor pathways in LPS-treated cells reflects their pivotal role in innate immune activation.[53–56] CSE's suppression of CD14 and CCL3L3 (key mediators of LPS-TLR4 signaling) and upregulation of CARD6 and ERBIN (negative regulators of inflammation) suggest a dual mechanism: dampening pro-inflammatory signals while enhancing resolution-phase responses. These findings are consistent with the observed reduction in cytokine secretion and oxidative stress.[57–60]

Despite these advances, limitations must be acknowledged. The study's reliance on an in vitro LPS model does not fully replicate the complexity of chronic lung diseases, which often involve persistent microbial colonization or autoimmune components. Additionally, while CSE's nucleoside and polysaccharide content likely underlies its bioactivity, further fractionation studies are needed to identify specific active compounds. Future work should validate these findings in animal models and assess the bioavailability of CSE components in vivo.

Conclusion

In summary, CSE exhibits potent anti-inflammatory and antioxidant properties in LPS-stimulated THP-1 macrophages. It suppresses pro-inflammatory cytokines (IL-6, TNF-α, IL-1β, IL-8), reduces oxidative stress via Nrf2/HO-1 activation, and modulates critical immune pathways, including Toll-like and NOD-like receptor signaling. The protective effects of CSE on BEAS-2B cells in a co-culture system further highlight its potential to mitigate inflammatory cross-talk in the respiratory epithelium. These results position Cordyceps sinensis as a promising candidate for developing nutraceuticals aimed at managing inflammatory lung conditions. Future studies should focus on in vivo validation and clinical translation to harness its full therapeutic potential.

Data Sharing Statement

The datasets analyzed and used in this study are available via corresponding author on reasonable request.

Consent for Publication

All authors have confirmed and agreed to publish this manuscript.

Acknowledgments

We are grateful to Professor Shulei Han for his technical support in the analysis of extracts, and to Dr. Zhen Ni for his technical support in the data analysis of transcriptome.

Author Contributions

All authors made a significant contribution to the work reported, whether that is in the conception, study design, execution, acquisition of data, analysis and interpretation, or in all these areas; took part in drafting, revising or critically reviewing the article; gave final approval of the version to be published; have agreed on the journal to which the article has been submitted; and agree to be accountable for all aspects of the work.

Funding

This work was supported by the Mechanisms and Applications of Cordyceps sinensis in Respiratory and Immune Systems (202315010534-JS-286).

Disclosure

The authors report no conflicts of interest in this work.

References

1. Aware CB, Patil DN, Suryawanshi SS, et al. Natural bioactive products as promising therapeutics: a review of natural product-based drug development. *S Afr J Bot*. 2022;151:512–528. doi:10.1016/j.sajb.2022.05.028
2. Nestler G. Traditional Chinese medicine. *Mcna*. 2002;86:63–73.
3. Normile D. The new face of traditional Chinese medicine. *Science*. 2003;10:188–190. doi:10.1126/science.299.5604.188
4. Chen YC, Chen YH, Pan BS, et al. Functional study of Cordyceps sinensis and cordycepin in male reproduction: a review. *J Food Drug Anal*. 2017;25:197–205. doi:10.1016/j.jfda.2016.10.020
5. Liu W, Gao Y, Zhou Y, et al. Mechanism of cordyceps sinensis and its extracts in the treatment of diabetic kidney disease: a review. *Front Pharmacol*. 2022;13:881835. doi:10.3389/fphar.2022.881835
6. Xiao Y, Zhang X, Huang Q. Protective effects of Cordyceps sinensis exopolysaccharide-selenium nanoparticles on H2O2-induced oxidative stress in HepG2 cells. *Int J Biol Macromol*. 2022;31:339–351. doi:10.1016/j.ijbiomac.2022.05.173
7. Sung GH, Hywel Jones NL, Sung JM, et al. Phylogenetic classification of Cordyceps and the clavicipitaceous fungi. *Stud Mycol*. 2007;57:5–59. doi:10.3114/sim.2007.57.01
8. Zhang Y, Liu J, Wang Y, et al. Nucleosides and amino acids, isolated from Cordyceps sinensis, protected against cyclophosphamide-induced myelosuppression in mice. *Nat Prod Res*. 2022;36:6056–6059. doi:10.1080/14786419.2022.2043307
9. Dong Z, Sun X. Chemical components in cultivated Cordyceps sinensis and their effects on fibrosis. *Chi Herb Med*. 2023;16:162–167.
10. Shu X, Xu D, Qu Y, et al. Efficacy and safety of Cordyceps sinensis (Hirsutella sinensis, Cs-C-Q80) in chronic bronchitis. *Front Pharmacol*. 2024;13:1428216. doi:10.3389/fphar.2024.1428216
11. Yao L, Zhu L, Chen C, et al. A systematic review on polysaccharides from fermented Cordyceps sinensis: advances in the preparation, structural characterization, bioactivities, structure-activity relationships. *Int J Bio Macromol*. 2024;5:137275. doi:10.1016/j.ijbiomac.2024.137275
12. Liu Y, Wang J, Wang W, et al. The chemical constituents and pharmacological actions of Cordyceps sinensis. *Evid Based Complement Alternat Med*. 2015;1:575063.
13. Chen L, Alabdullah M, Mahnke K. Adenosine, bridging chronic inflammation and tumor growth. *Front Immunol*. 2023;31:1258637. doi:10.3389/fimmu.2023.1258637
14. Antonioli L, Pacher P, Haskó G. Adenosine and inflammation: it's time to (re) solve the problem. *Trends Pharmacol Sci*. 2022;43:43–55. doi:10.1016/j.tips.2021.10.010
15. Pasquini S, Contri C, Borea PA, et al. Adenosine and inflammation: here, there and everywhere. *Int J Mole Sci*. 2021;19:7685. doi:10.3390/ijms22147685
16. Paladines N, Dawson S, Ryan W, et al. Metabolic reprogramming through mitochondrial biogenesis drives adenosine anti-inflammatory effects: new mechanism controlling gingival fibroblast hyper-inflammatory state. *Front immunol*. 2023;7:1148216. doi:10.3389/fimmu.2023.1148216
17. Chen L, Liu X, Zheng K, et al. Cordyceps polysaccharides: a review of their immunomodulatory effects. *Molecules*. 2024;29:5107. doi:10.3390/molecules29215107
18. Li B, Zhang J, Liu Y, et al. Characterization, antioxidant capacity and protective effect of peptides from cordyceps militaris cultivated with tussah pupa on oxidative injured HepG2 cells. *J Microbiol Biotechnol*. 2024;28:1082–1091. doi:10.4014/jmb.2312.12012
19. Zhang Y, Li K, Zhang C, et al. Research progress of cordyceps sinensis and its fermented mycelium products on ameliorating renal fibrosis by reducing epithelial-to-mesenchymal transition. *J Inflamm Res*. 2023;7:2817–2830. doi:10.2147/JIR.S413374
20. Song J, Wang Y, Liu C. Liu C, et al.Cordyceps militaris fruit body extract ameliorates membranous glomerulonephritis by attenuating oxidative stress and renal inflammation via the NF-κB pathway. *Food Funct*. 2016;7:2006–2015. doi:10.1039/C5FO01017A
21. Zheng Y, Li L, Cai T. Cordyceps polysaccharide ameliorates airway inflammation in an ovalbumin-induced mouse model of asthma via TGF-β1/Smad signaling pathway. *Respir Physiol Neurobiol*. 2020;276:103412. doi:10.1016/j.resp.2020.103412
22. Chen S, Wang J, Dong N, et al. Polysaccharides from natural Cordyceps sinensis attenuated dextran sodium sulfate-induced colitis in C57BL/6J mice. *Food Funct*. 2023;14:720–733. doi:10.1039/D2FO02555H
23. Arias-Pérez RD, Taborda NA, Gómez DM, et al. Inflammatory effects of particulate matter air pollution. *Environ Sci Pollut Res Int*. 2020;27:42390–42404. doi:10.1007/s11356-020-10574-w
24. Niranjan R, P MK, Tripathi SN, et al. Proliferation of lung epithelial cells is regulated by the mechanisms of autophagy upon exposure of soots. *Front Cell Dev Bio*. 2021;21:662597. doi:10.3389/fcell.2021.662597
25. Vanka KS, Shukla S, Gomez HM, et al. Understanding the pathogenesis of occupational coal and silica dust-associated lung disease. *Eur Respir Re*. 2022;12:31.
26. Bykov V, Pavlov K, Popov V, et al. Surgical treatment of lung injuries and diseases in patients with blunt chest trauma. *Khirurgiia*. 2020;12:64–69.
27. Lee JW, Chun W, Lee HJ, et al. The role of macrophages in the development of acute and chronic inflammatory lung diseases. *Cells*. 2021;14:897. doi:10.3390/cells10040897
28. Bocchino M, Zanotta S, Capitelli L, et al. Dendritic cells are the intriguing players in the puzzle of idiopathic pulmonary fibrosis pathogenesis. *Front Immunol*. 2021;30(12):664109. doi:10.3389/fimmu.2021.664109
29. Bu T, Wang LF, Yin YQ. How do innate immune cells contribute to airway remodeling in COPD progression? *Int J Chron Obstruct Pulmon Dis*. 2020;10:107–116. doi:10.2147/COPD.S235054
30. Rambacher KM, Monir NH. Cysteine redox state regulates human β2-adrenergic receptor binding and function. *Sci Rep*. 2020;19:2934. doi:10.1038/s41598-020-59983-4
31. Cong B, Dong X, Yang Z, et al. Single-cell spatiotemporal analysis of the lungs reveals Slamf9+ macrophages involved in viral clearance and inflammation resolution. *Cell Discov*. 2024;16:104. doi:10.1038/s41421-024-00734-4
32. Li J, Lu K, Sun F, et al. Panaxydol attenuates ferroptosis against LPS-induced acute lung injury in mice by Keap1-Nrf2/HO-1 pathway. *J Transl Med*. 2021;19:96. doi:10.1186/s12967-021-02745-1

33. Wang R, Liu S, Shen S, et al. Protective mechanism of Cordyceps sinensis treatment on acute kidney injury-induced acute lung injury through AMPK/mTOR signaling pathway. *Chin J Integr Med*. 2023;29:875–884. doi:10.1007/s11655-023-3593-4
34. Zhang M, Sun X, Miao Y, et al. Cordyceps cicadae and Cordyceps gunnii have closer species correlation with Cordyceps sinensis: from the perspective of metabonomic and MaxEnt models. *Sci Rep*. 2020;28:20469.
35. Liu D, Li J, Li Y, et al. Status of global macrofungal conservation based on red lists and suggestions for a comprehensive strategy in China. *Acta Edulis Fungi*. 2021;28:108–114.
36. Bang Y, Hwang S, Kim YE, et al. Therapeutic efficacy of thrombin-preconditioned mesenchymal stromal cell-derived extracellular vesicles on Escherichia coli-induced acute lung injury in mice. *Respir Res*. 2024;7:303. doi:10.1186/s12931-024-02908-w
37. Cabrer Rivera GL, Madera Sandoval RL, León Pedroza JI, et al. Increased TNF-α production in response to IL-6 in patients with systemic inflammation without infection. *Clin Exp Immunol*. 2022;19:225–235. doi:10.1093/cei/uxac055
38. Wang R, Li Q, Wu P, et al. Fe-capsaicin nanozymes attenuate sepsis-induced acute lung injury via NF-κB signaling. *Int j Nanomed*. 2024;2024:73–90. doi:10.2147/IJN.S436271
39. Wu Y, Ying J, Zhu X, et al. Pachymic acid suppresses the inflammatory response of chondrocytes and alleviates the progression of osteoarthritis via regulating the Sirtuin 6/NF-κB signal axis. *Int Immunopharmacol*. 2023;124:110854. doi:10.1016/j.intimp.2023.110854
40. Liu J, Wang Y, Heelan WJ, et al. Mucoadhesive probiotic backpacks with ROS nanoscavengers enhance the bacteriotherapy for inflammatory bowel diseases. *Sci Adv*. 2022;11:eabp8798. doi:10.1126/sciadv.abp8798
41. Wang Y, Wang Y, Ma J, et al. YuPingFengSan ameliorates LPS-induced acute lung injury and gut barrier dysfunction in mice. *J Ethnopharmacol*. 2023;10:116452. doi:10.1016/j.jep.2023.116452
42. Cho YE, Kim Y, Kim SJ, et al. Overexpression of interleukin-8 promotes the progression of fatty liver to nonalcoholic steatohepatitis in mice. *Int J Mol Sci*. 2023;23:15489. doi:10.3390/ijms242015489
43. Favaro F, Lucian Mateo F, Moreno Caceres J, et al. TRAIL receptors promote constitutive and inducible IL-8 secretion in non-small cell lung carcinoma. *Cell Death Dis*. 2022;15:1046. doi:10.1038/s41419-022-05495-0
44. Yabluchanskiy A, Ma Y, Iyer RP, et al. Matrix metalloproteinase-9: many shades of function in cardiovascular disease. *Physiology*. 2013;28 (6):391–403. doi:10.1152/physiol.00029.2013
45. Sarkar J, Nandy SK, Chowdhury A, Chakraborti T, Chakraborti S. Inhibition of MMP-9 by green tea catechins and prediction of their interaction by molecular docking analysis. *Biomed Pharmacother*. 2016;84:340–347. doi:10.1016/j.biopha.2016.09.049
46. Cheng J, Zhang Y, Ma L, et al. Macrophage-derived extracellular vesicles-coated palladium nanoformulations modulate inflammatory and immune homeostasis for targeting therapy of ulcerative colitis. *Adv Sci*. 2023;10:2304002. doi:10.1002/advs.202304002
47. Qi Z, Yang W, Xue B, et al. ROS-mediated lysosomal membrane permeabilization and autophagy inhibition regulate bleomycin-induced cellular senescence. *Autophagy*. 2024;20:2000–2016. doi:10.1080/15548627.2024.2353548
48. Zhang Y, Zhou L, Cheng G, et al. Cordyceps sinensis ameliorates idiopathic pulmonary fibrosis in mice via inhibiting mitochondrion-mediated oxidative stress. *Medcomm–Future Med*. 2024;3:e91. doi:10.1002/mef2.91
49. Huang Y, Wang A, Jin S, et al. Activation of the NLRP3 inflammasome by HMGB1 through inhibition of the Nrf2/HO-1 pathway promotes bleomycin-induced pulmonary fibrosis after acute lung injury in rats. *Allergologia Immunopathol*. 2023;1:56–67. doi:10.15586/aei.v51i3.668
50. Stagg J, Golden E, Wennerberg E, et al. The interplay between the DNA damage response and ectonucleotidases modulates tumor response to therapy. *Sci Immunol*. 2023;14:eabq3015. doi:10.1126/sciimmunol.abq3015
51. Rosa PB, Bettio LEB, Neis VB, et al. The antidepressant-like effect of guanosine is dependent on GSK-3β inhibition and activation of MAPK/ERK and Nrf2/heme oxygenase-1 signaling pathways. *Purinergic Signalling*. 2019;15:491–504. doi:10.1007/s11302-019-09681-2
52. Sha W, Zhao B, Wei H, et al. Astragalus polysaccharide ameliorates vascular endothelial dysfunction by stimulating macrophage M2 polarization via potentiating Nrf2/HO-1 signaling pathway. *Phytomedicine*. 2023;112:154667. doi:10.1016/j.phymed.2023.154667
53. Liu Y, Shang L, Zhou J, et al. Emodin attenuates LPS-induced acute lung injury by inhibiting NLRP3 inflammasome-dependent pyroptosis signaling pathway in vitro and in vivo. *Inflammation*. 2022;45(2):753–767. doi:10.1007/s10753-021-01581-1
54. Wang JL, Luo X, Liu L. Targeting CARD6 attenuates spinal cord injury (SCI) in mice through inhibiting apoptosis, inflammation and oxidative stress associated ROS production. *Aging*. 2019;11(24):12213. doi:10.18632/aging.102561
55. Liu Y, Fang Q, Ming T, et al. Knockout of Erbin promotes pyroptosis via regulating NLRP3/caspase-1/Gasdermin D pathway in sepsis-induced acute kidney injury. *Clin Exp Nephrol*. 2023;27:781–790. doi:10.1007/s10157-023-02364-8
56. Duan T, Du Y, Xing C, et al. Toll-like receptor signaling and its role in cell-mediated immunity. *Front Immunol*. 2022;3:812774.
57. Yj F, Xu B, Huang S-W. Huang Sw, et al.Baicalin prevents LPS-induced activation of TLR4/NF-κB p65 pathway and inflammation in mice via inhibiting the expression of CD14. *Acta Pharmacol Sin*. 2021;42:88–96. doi:10.1038/s41401-020-0411-9
58. Lara S, Akula S, Fu Z, et al. The human monocyte—A circulating sensor of infection and a potent and rapid inducer of inflammation. *Int J mol Sci*. 2022;31:3890. doi:10.3390/ijms23073890
59. Peluso I, Magrone T, Dv V, et al. Antioxidant, anti-inflammatory, and microbial-modulating activities of nutraceuticals and functional foods. *Oxid Med Cell Longev*. 2017;2017:7658617. doi:10.1155/2017/7658617
60. Damián MR, Cortes Perez NG, Quintana ET, et al. Functional foods, nutraceuticals and probiotics: a focus on human health. *Microorganisms*;2022. 1065. doi:10.3390/microorganisms10051065